Vol 18 No 9, September 2009
1674-1056/2009/18(09)/3900-05

Chinese Physics B

© 2009 Chin. Phys. Soc.
and IOP Publishing Ltd

High-speed 2 × 2 silicon-based electro-optic switch with nanosecond switch time*

Xu Xue-Jun(徐学俊)†, Chen Shao-Wu(陈少武), Xu Hai-Hua (徐海华),
Sun Yang(孙 阳), Yu Yu-De(俞育德), Yu Jin-Zhong(余金中), and Wang Qi-Ming(王启明)

State Key Laboratory on Integrated Optoelectronics, Institute of Semiconductors, Chinese Academy of Sciences, Beijing 100083, *China*

(Received 26 December 2008; revised manuscript received 27 March 2009)

A 2 × 2 electro-optic switch is experimentally demonstrated using the optical structure of a Mach–Zehnder interferometer (MZI) based on a submicron rib waveguide and the electrical structure of a PIN diode on silicon-on-insulator (SOI). The switch behaviour is achieved through the plasma dispersion effect of silicon. The device has a modulation arm of 1 mm in length and cross-section of 400 nm×340 nm. The measurement results show that the switch has a $V_\pi L_\pi$ figure of merit of 0.145 V·cm and the extinction ratios of two output ports and cross talk are 40 dB, 28 dB and −28 dB, respectively. A 3 dB modulation bandwidth of 90 MHz and a switch time of 6.8 ns for the rise edge and 2.7 ns for the fall edge are also demonstrated.

Keywords: silicon-on-insulator, electro-optic switch, plasma dispersion effect, switch time
PACC: 4280L, 4282, 4280S

1. Introduction

As essential components in opto-electronics integration circuits (OEIC) and on-chip optical interconnection systems, high-speed electro-optic modulators and switches have gained more and more attention among silicon photonic devices. They are used to put high-speed analogue or digital electrical signals onto continuous optical carrier waves. Because silicon is a kind of semiconductor with centrosymmetric crystal structure, its linear electro-optic (Pockels) coefficient vanishes. Silicon-based modulators and switches are often based on the free carrier plasma dispersion effect.[1] Therefore, the modulation speed or switch time is primarily limited by carrier transport processes in the semiconductor. With a forward-biased PIN injected structure, carrier diffusion is dominant, and thus the modulation speed is not so high, typically ∼20 MHz based on rib waveguides with large cross-sections,[2] while in a MOS capacitor or reverse-biased PN junction, carrier drift under high electrical field is dominant. This leads to much higher modulation speeds; for example, a 10 GHz modulator based on a MOS capacitor[3] and a 20 GHz modulator based on a reverse-biased PN junction[4] have been experimentally demonstrated. However, the modulation efficiency of these devices is much smaller than PIN injected ones and they are more complicated to fabricate. The device lengths are often in the order of several centimetres. Fortunately, using nanophotonic waveguides with submicron cross-sections, the transport distance can be shortened significantly in forward-biased PIN diodes, and thus modulation speeds higher than 1 GHz can be also achieved.[5]

In this paper we report a high-speed 2 × 2 PIN injected Mach–Zehnder electro-optic switch with nanosecond switch time. The device is fabricated with a series of aligned electron beam and photolithography steps. Measurement results show that the modulation efficiency figure of merit $V_\pi L_\pi$ is 0.145 V·cm and the transient rise and fall time are 6.8 ns and 2.7 ns, respectively. Some other results are also reported.

2. Device design and fabrication

The electro-optic switch is designed with the optical structure of a 2 × 2 Mach–Zehnder interferometer (MZI) and the electrical structure of a PIN diode. The MZI consists of two identical 2 × 2 multimode

*Project supported by the National Natural Science Foundation of China (Grant No 60577044), the State Key Development Program for Basic Research of China (Grant No 2007CB613405) and the National High Technology Research and Development Program of China (Grant No 2006AA032424).
†E-mail: xjxu@semi.ac.cn

interference (MMI) couplers and two long arms with submicron rib waveguides with the same length. After input into MMI, the light from one of the input ports is split into two beams which propagate in their own arm. These two beams have the same intensity but a phase difference of $\pi/2$ (the beam in the cross port lags). As the MZI has identical arm lengths, the two equal beams arrive at the output MMI with the same $\pi/2$ phase difference. Then the behaviour of output MMI is the same as the input MMI, except that their input and output ports are exchanged. Therefore all the light propagates through the cross port of the MZI (cross state). With a PIN diode in one arm of the MZI, carriers can be injected into the waveguide under forward bias. Thus the refractive index and absorption coefficient will change due to the plasma dispersion effect, and follow the relationships below:[1]

$$\Delta n = -8.8 \times 10^{-22} \Delta N_{\mathrm{e}} - 8.5 \times 10^{-18} (\Delta N_{\mathrm{h}})^{0.8},$$
$$\Delta \alpha = 8.5 \times 10^{-18} \Delta N_{\mathrm{e}} + 6.0 \times 10^{-18} \Delta N_{\mathrm{h}}, \qquad (1)$$

where Δn and $\Delta \alpha$ are the changes of the refractive index and absorption coefficient, and ΔN_{e} and ΔN_{h} are the changes of the carrier concentration of electrons and holes, respectively. Then the two equal beams propagating in the arms of the MZI will experience different phase shifts. If the phase difference achieves π, all the light will propagate through the bar port of the MZI (bar state). In this way the switch behaviour is realized.

With a thin 100 nm slab, the rib waveguide on each arm is 340 nm in height, 400 nm in width. These parameters are chosen to ensure that the waveguide satisfies the single-mode condition.[6] The length of the modulation area is 1000 μm. Compared to directional couplers, MMIs can provide wide optical bandwidth and large fabrication tolerance. The two 2×2 MMIs have the same waveguide width of 6 μm, and their lengths and the positions of the input/output waveguides are optimized through numerical simulations in order to achieve good power balance and low extra loss. The tapered input and output waveguides are used to reduce optical reflection at the waveguide discontinuities. The PIN diode is formed across the waveguide, with a heavily doped area on its slab and an intrinsic area in the waveguide core. A schematic of the device is shown in Fig.1(a), together with the cross-section of the modulation area. The heavily doped regions are 1.5 μm away from the edge of the waveguide core in order to reduce absorption loss due to the overlap of the optical mode and the optically absorbing heavily doped regions. However, it will take a longer time for carriers transporting to cross the waveguide due to this long distance, hence the modulation speed is not as high as that reported by IBM.[5]

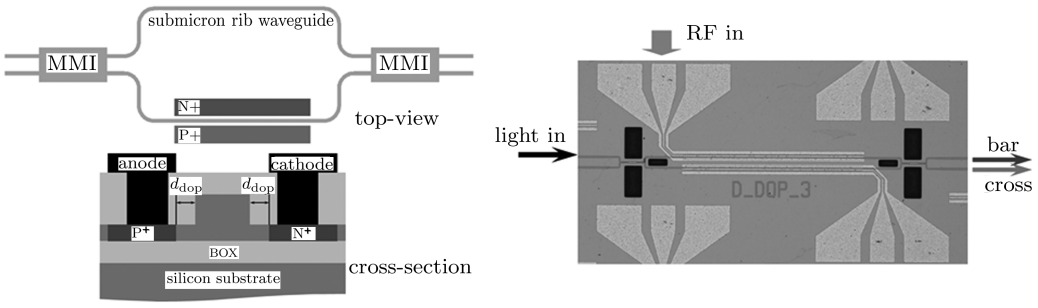


Fig.1. (a) A schematic of the PIN-MZI electro-optic switch; (b) The microscope image of a fabricated device with a modulation arm length of 1000 μm.

We fabricated the devices on a SOI wafer with a top silicon layer of 340 nm thickness and a BOX layer of 2 μm thickness from SOITEC.[7] The submicron rib waveguide and MZI are defined using electron-beam lithography (EBL).[8] Then 240 nm thick silicon is etched using an inductively coupled plasma (ICP) dry etcher, leaving a slab 100 nm thick. After that, two steps of aligned photolithography are used to define the ion implantation windows. The boron ions, with energy of 10 keV and dose of 8.0×10^{14} cm^{-2} and phosphorus ions, with energy of 20 keV and dose of 2.0×10^{15} cm^{-2}, are implanted to form the P and N heavily doped areas, respectively. Then a 500 nm thick SiO_2 layer is deposited on the device by plasma

enhanced chemical vapour deposition (PECVD), followed by a rapid thermal anneal (RTA) for 10 seconds at 1050 °C, to activate the implanted dopants. Then via holes for metal contacts are formed by photolithography and SiO_2 ICP etch. After the silicon is exposed, a thin layer of Ti is evaporated onto the surface and annealed in N_2 atmosphere for 1 min at 800^oC to form the $TiSi_2$ contact layer and TiN barrier layer. A thick layer of aluminium is then evaporated and used to form coplanar transmission line electrodes through photolithography and wet etching. A microscope image of a fabricated switch is shown in Fig.1(b). The devices are then diced and cut by a lithography-based method[9] to form the waveguide facets for measurements.

3. Measurement results

We measured both the static and dynamic performances of the electro-optic switches. The TE-polarized light with a power of 15 dBm is launched into one of the input ports of the switch through a tapered-lensed fibre. The output light is also coupled through a similar fibre into an optical powermeter. The operation optical wavelength is 1.55 μm. Figure 2(a) shows the output optical power of both bar and cross ports with different bias voltages. As the voltage increases from 0.93 V to 1.45 V, the output power of the cross port decreases from maximum to minimum and the output power of the bar port increases from minimum to maximum. This indicates that the output light is switched from the cross port to the bar port. Thus the $V_\pi L_\pi$ is 0.145 V·cm for the device. The optical structure of the switch shows great performance. The extinction ratios of the bar and cross ports are 40 dB and 28 dB respectively and the cross talk between the two ports is −28 dB. The large extinction ratios and small cross talk come from the good power balance of the input and output MMI splitter and coupler. It is worth noting that the output of the bar port is not extinct while no voltage is applied to the device. This may result from asymmetry of the two arms of the MZI due to fabrication error. However, this can be improved by shifting the optical wavelength to a proper value. We also measured the current–voltage characteristics of the PIN diode in one arm of the switch, as shown in Fig.2(b). From the curve we can obtain that the DC power consumption of the switch is as small as 9.4 mW. Also, the forward differential resistance of the PIN diode is ∼70 Ω after the diode is turned on. This large resistance may lead to impedance mismatch to drive electronics and measurement instruments, thus deteriorating the frequency response of the device. In order to reduce the resistance, the contact resistance of the metal electrode to the heavily doped region and the doping concentration should be optimized further.

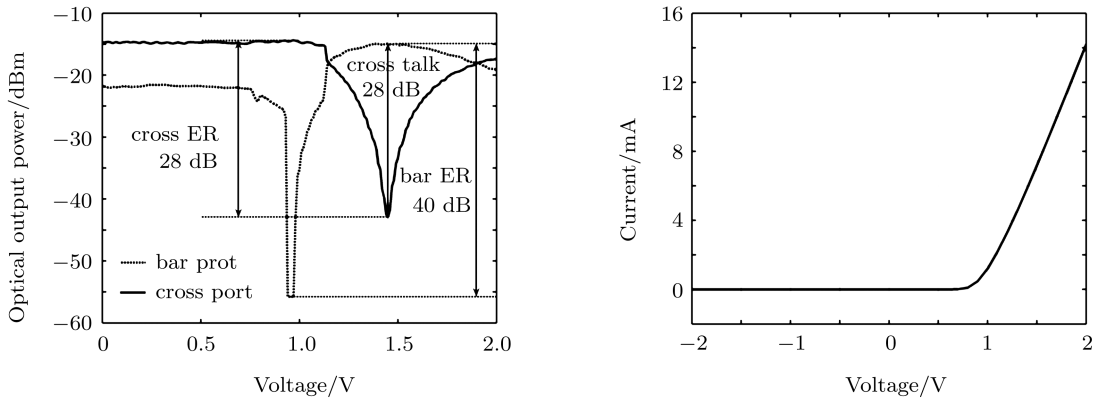


Fig.2. (a) The output optical power of the bar and cross ports of the switch versus applied bias voltage; (b) *I–V* curve of the PIN diode in one arm of the PIN-MZI switch.

The dynamic performance of the switch is first characterized by small signal frequency response. We apply a 1.2 V DC bias on the switch to ensure the device is operating in the linear-modulated region. Then

an RF signal with a power of −1 dBm is also applied on the device through a bias-tee. The optical output is coupled into a 12 GHz high-speed detector and then into an electrical frequency spectrum analyser. The RF frequency sweep is performed from 1 MHz to 1 GHz. The frequency response of the switch is shown in Fig.3, indicating a 3 dB bandwidth of about 90 MHz.

The switch time is measured by application of a pulsed electrical signal on the device. The rise/fall time of the pulsed signal is less than 1 ns and the amplitude is set to V_π. The switch output is first directed to a high-speed detector with a maximum conversion gain of −600 V/W for opto-eletronic conversion and then displayed by the oscilloscope, as shown in Fig.4. The 10%–90% rise and fall time are 6.8 ns and 2.7 ns, respectively. In the rise edge, carriers are injected into the intrinsic region of the PIN diode. Diffusion due to the nonuniform concentration distributions dominates in carrier transportation. In the fall edge, carriers are depleted in the intrinsic region. Drift under electric field dominates in this procedure. The drift velocity of carriers is often much higher than the diffusion velocity. That is why the rise time is much longer than the fall time.

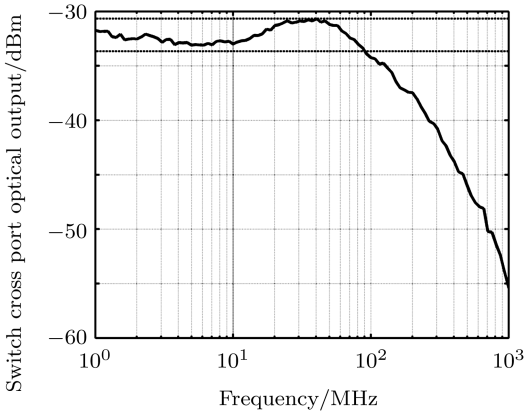
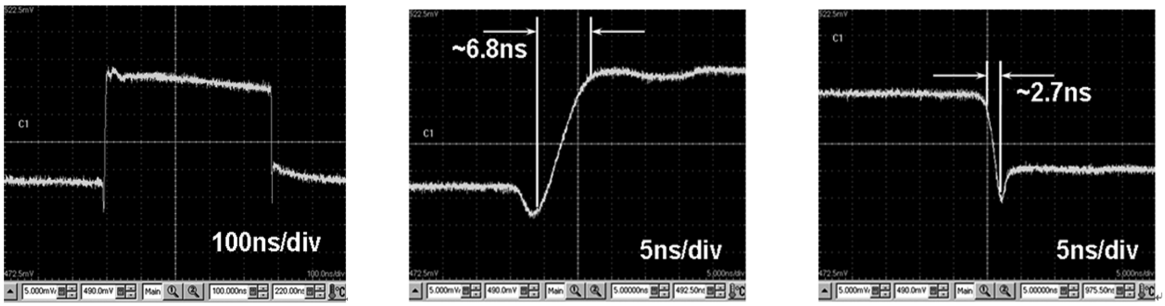


Fig.3. The frequency response of the switch, measured at the cross port, with frequency sweep from 1 MHz to 1 GHz.



(a) (b) (c)

Fig.4. (a) The pulse response of the switch displayed by the oscilloscope, (b) the rise edge, (c) the fall edge.

Compared to other PIN injected silicon nanophotonics devices,[5,10,11] this is the first electro-optical switch with two input and two output ports. Our device has a relatively high modulation efficiency - figure of merit $V_\pi L_\pi$ of 0.145 V·cm. By shortening the length of the modulation arms, the $V_\pi L_\pi$ can be decreased further. Although the modulation speed is comparable to that of the MIT injection modulator,[10] the static extinction ratio is larger than those of previous reported devices.[5] This is due to our careful design for the optical structure. As mentioned above, the switch time is significantly dependent on the carrier transport distance across the waveguide. By shortening the distance between the edge of the heavily doped region and the waveguide ridge $d_{\rm dop}$, we can reduce the switch time. Theoretical simulation results indicate that the rise time can be reduced by 61% and the fall time by 83% when $d_{\rm dop}$ is decreased from 1.5 μm to 0.3 μm. In addition, carrier lifetime reduction is another efficient way to reduce the switch time.[11] The carrier lifetime in the intrinsic region of the PIN diode can be reduced by helium,[12] oxygen,[13] silicon[14] or some other ion implantation. Taking these two improvements together, it is possible to realize a silicon-

based electro-optic switch with switch time less than 1 ns.

4. Conclusion

We report a 2 × 2 PIN injected Mach–Zehnder interferometer based electro-optic switch with a few nanoseconds switch time. The device is based on SOI submicron rib waveguides and thus shows good static and dynamic performance. The measured modulation efficiency figure of merit $V_\pi L_\pi$ is 0.145 V·cm for the 1000 μm long MZI arm and the extinction ratios of the bar and cross ports are 40 dB and 28 dB respectively; the cross talk between the two ports is −28 dB. The DC power consumption is only 9.4 mW. A small signal frequency sweep shows that the 3 dB modulation bandwidth is about 90 MHz, and the rise and fall time is 6.8 ns and 2.7 ns by application of a pulse electrical signal on the device. The switch time can be reduced further through shortening the distance between the edge of the heavily doped region and the waveguide ridge and the carrier lifetime.

Acknowledgements

The authors are grateful to Yang Fuhua, Ji An, Bai Yunxia, Han Weihua, Fan Zhongchao, Li Yan, Xu Jiadong, Wang Desong, Hu Chuanxian, and Pan Lingfeng in the Semiconductor Integration Technology Engineering Center, Zheng Jun in the State Key Laboratory on Integrated Optoelectronics, Institute of Semiconductors, Chinese Academy of Sciences, Beijing, China, Du Meng in the Institute of Microelectronics, Chinese Academy of Sciences, Beijing, for their help in the device fabrication.

References

[1] Soref R A and Bennett B R 1987 *IEEE J. Quantum Electron.* **23** 123
[2] Irace A, Coppola G, Iodice M and Cutolo A 1999 *SPIE* **3847** 94
[3] Liao L, Samara-Rubio D, Morse M, Liu A, Hodge D, Rubin D, Keil U D and Franck T 2005 *Opt. Express* **13** 3129
[4] Liu A, Liao L, Rubin D, Nguyen H, Ciftcioglu B, Chetrit Y, Izhaky N and Paniccia M 2007 *Opt. Express* **15** 660
[5] Green W M J G, Rooks M J, Sekaric L and Vlasov Y A 2007 *Opt. Express* **15** 17106
[6] Xu X, Chen S, Yu J and Tu X 2009 *J. Opt.* A: *Pure Appl. Opt.* **11** 015508
[7] SOITEC, Parc Technologique des Fontaines, 38190 Bernin, France, http://www.soitec.com
[8] Tang H X, Zuo Y H, Yu J Z and Wang Q M 2007 *Chin. Phys.* **16** 2011
[9] Xu X, Chen S, Li Z, Yu Y and Yu J 2008 *IEEE 5th Int. Conf. on Group IV Photonics* WP22, Sorrento, Italy
[10] Gan F, Spector S J, Geis M W, Grein M E, Schulein R T, Yoon J U, Lyszczarz T M and Kartner F X 2007 *Conference on Lasers and Electro-Optics/Quantum Electronics and Laser Science* Technical Digest, CTuQ6
[11] Zhou G, Geis M W, Spector S J, Gan F, Grein M E, Schulein R T, Orcutt J S, Yoon J U, Lennon D M, Lyszczarz T M, Ippen E P and Kartner F X 2008 *Opt. Express* **16** 5218
[12] Liu Y and Tsang H K 2006 *Opt. Lett.* **31** 1714
[13] Waldow M, Plotzing T, Gottheil M, Forst M, Bolten J, Wahlbrink T and Kurz H 2008 *Opt. Express* **16** 7693
[14] Wright N M, Thomson D J, Litvinenko K L, Headley W R, Smith A J, Knights A P, Gardes F Y, Mashanovich G Z, Gwilliam R and Reed G T 2008 *IEEE 5th Int. Conf. on Group IV Photonics* WP17, Sorrento, Italy